JOURNAL OF AIRCRAFT
Vol. 29, No. 4, July–Aug. 1992

Predicted Pressure Distribution on a Prop-Fan Blade Through Euler Analysis

Makoto Kobayakawa*
Kyoto University, Kyoto 606, Japan
Ryoji Takaki†
National Aerospace Laboratory, Chofu 182, Japan
Yoshifumi Kawakami‡
Sumitomo Precision Products Ltd., Amagasaki 660, Japan
and
Frederick B. Metzger§
Hamilton Standard, Windsor Locks, Connecticut 06096

Applicability of a numerical code to aerodynamic design of a prop-fan is established by precise agreement of numerical results with experimental data, i.e., not only measured integrated performance indices, such as power coefficient or net efficiency, but also pressure distribution on the blade surface should agree well with computed results. For this purpose, a Euler Code using the Total Variation Diminishing scheme has been developed. Numerical calculations are performed with this scheme for the SR-7L Prop-Fan at the freestream Mach number 0.5 and 0.78. The computed power coefficient, C_P = 0.34 at M_∞ = 0.5 shows good agreement with experimental data. At this computed C_P, the computed pressure distributions on the blade surfaces show good agreement with the experimental results. For the 0.78M_∞ case the computed C_P of 0.23 also shows good agreement with the experimental results, and the computed pressure distributions are in general agreement with the experimental data. These results indicate that the present Euler-Code could provide guidance for aerodynamic design of a Prop-Fan of the SR-7L type.

Nomenclature

b	=	blade chord
C_{LD}	=	design lift coefficient at each radial direction
C_P	=	power coefficient
c	=	speed of sound
c_p	=	pressure coefficient
D	=	diameter of the prop-fan
$\boldsymbol{E}, \boldsymbol{F}, \boldsymbol{G}, \boldsymbol{H}$	=	flux vectors
e	=	energy of unit volume
h	=	maximum thickness of an airfoil
J	=	transformation Jacobian
p	=	pressure
$\boldsymbol{Q}$	=	vector of conserved quantities
R	=	tip radius
R_1, R_2	=	Riemann invariants
r	=	section radius
S	=	entropy
U, V, W	=	contravariant velocity components
u, v, w	=	cylindrical velocity components
z, r, ϕ	=	cylindrical coordinates
β	=	blade angle at $0.75r/R$
γ	=	ratio of specific heats
$\Delta\theta$	=	blade twist angle at $0.75r/R$
Λ	=	sweep angle at 50% chord
ξ, η, ζ	=	coordinates of conformal mapping
ρ	=	air density
ψ	=	cone angle
Ω	=	angular velocity of rotation

Subscript

∞	=	freestream

Received March 7, 1991; revision received June 21, 1991; accepted for publication July 29, 1991.

*Associate Professor, Department of Aeronautical Engineering. Member AIAA.
†Researcher, Computational Sciences Division.
‡Manager, Aerospace R & D Department. Member AIAA.
§Chief of Propulsion Analysis, United Technologies Corporation, Member AIAA.

Introduction

DURING the 13 years since the prop-fan technology projects started as a new conceptual propulsion system, many experiments in wind tunnels and on a flying test bed (FTB) have been performed, mainly in the United States. At the same time, in the last decade rapid progress has been made in computational aerodynamics, and many papers about applying this work to the prop-fan have been published. The authors also presented several kinds of computational results by use of the Vortex Lattice Method (VLM),[1] potentional analysis,[2] Euler and Navier-Stokes analyses[2,3] for the prop-fan models.

However, in order to achieve the best prop-fan design it is necessary to examine the accuracy of numerical computations, not only to calculate integrated performance indices, such as efficiency and power coefficient, but to more precisely calculated phenomena on the blade, such as pressure distributions and the location of shock waves. If agreement in these more basic phenomena can be demonstrated at both cruise and takeoff conditions, then a prop-fan design could be optimized aerodynamically without wind-tunnel testing.

In this paper calculations were made using a Euler Code developed by the authors and compared to experimental results of SR-7L prop-fan published in an AIAA paper.[4] The Euler Code used employed the Total Variation Diminishing (TVD) scheme together with the Alternating Direction Implicit (ADI) algorithm. The objective was to show the agreement between predicted and measured blade surface pressures at different operating conditions. Good agreement would

establish the validity of the Euler Code for designing a prop-fan.

Euler Equations and Numerical Method

In the same manner as other developers of Euler Codes for prop-fans, nonorthogonal coordinate transformations of the governing equations are employed to map the surface of the nacelle and both sides of the blade onto constant coordinate surfaces. The basic orthogonal coordinate system is cylindrical with z oriented along the rotational axis, r extending radially outward from the z axis, and ϕ the meridional angle measured from a vertical plane. This is illustrated in Fig. 1. The cylindrical coordinate system is easier to apply for the rotating blade boundary conditions than the Cartesian coordinate system.

Under the assumption of inviscid compressible flow, the governing partial differential equation in the weak conservation law form is given by

$$\boldsymbol{Q}_t + \boldsymbol{E}_\xi + \boldsymbol{F}_\eta + \boldsymbol{G}_\zeta + \boldsymbol{H} = 0 \qquad (1)$$

where

$$\boldsymbol{Q} = \frac{1}{J}\begin{bmatrix} \rho \\ \rho u \\ \rho v \\ \rho w \\ e \end{bmatrix}, \boldsymbol{E} = \frac{1}{J}\begin{bmatrix} \rho U \\ \rho u U + p\xi_z \\ \rho v U + p\xi_r \\ \rho w U + p\xi_\phi / r \\ (e + p)U - p\xi_t \end{bmatrix}$$

$$\boldsymbol{F} = \frac{1}{J}\begin{bmatrix} \rho W \\ \rho u W + p\zeta_z \\ \rho v W + p\zeta_r \\ \rho w W + p\zeta_\phi / r \\ (e + p)W - p\zeta_t \end{bmatrix}, \boldsymbol{H} = \frac{1}{Jr}\begin{bmatrix} \rho v \\ \rho u v \\ \rho(v^2 - w^2) \\ 2\rho v w \\ (e + p)V \end{bmatrix}$$

$$e = \frac{p}{\gamma - 1} + \frac{\rho}{2}(u^2 + v^2 + w^2)$$

In the above equations, $\boldsymbol{H}$ contains centrifugal and Coriolis force terms due to the blade rotation. U, V, and W are contravariant velocity components, and J is the transformation Jacobian. The unknown variables, pressure p, density ρ, cylindrical velocity components u, v, and w are nondimensionalized by p_∞, ρ_∞, and $c_\infty/\sqrt{\gamma}$, respectively, where c_∞ is the freestream speed of sound and γ is the ratio of specific heats. Other quantities, time t and angular velocity Ω are nondimensionalized by $c_\infty/(D\sqrt{\gamma})$ and $D\sqrt{\gamma}/c_\infty$, respectively. Precise expressions for U, V, W, J, and metrics are found in Refs. 5 and 6.

The numerical algorithm used to solve the Euler equations in computational space is the noniterative, ADI schemes. The implicit procedure enhances the speed of convergence. Undesirable oscillations in the solution are suppressed, and resolution is improved by the TVD scheme. In this case, Harten's TVD scheme is used.[7]

Boundary Conditions

In order to obtain an accurate solution, the boundary conditions are carefully specified. The following boundary conditions should be imposed:

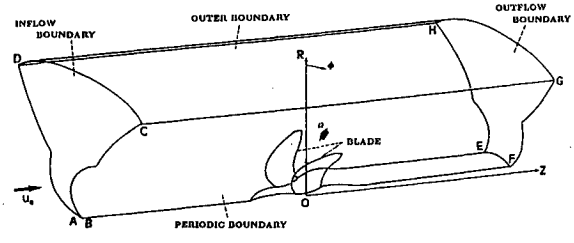

Fig. 1 Computational space around prop-fan.

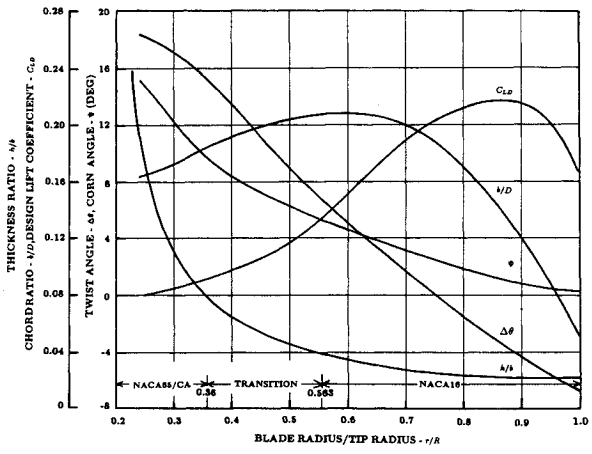

Fig. 2 Basic blade geometry.

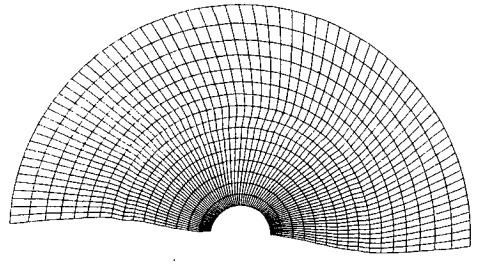

a) ξ-constant plane

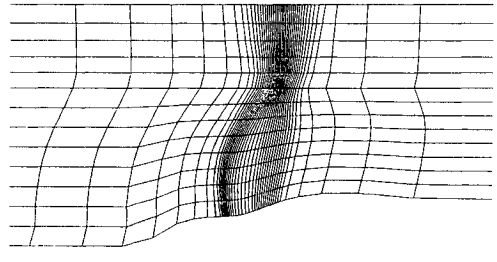

b) η-constant plane

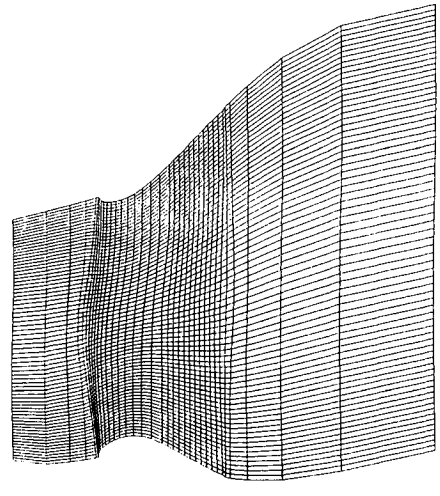

c) ζ-constant plane

Fig. 3 Computational grids around SR-7L prop-fan.

1) Conditions along the ξ direction: inflow and outflow conditions.

2) Conditions along the η direction: impermeable condition on the nacelle and outer boundary condition.

3) Conditions along the ζ direction: impermeable condition on the blades (including blade tip and trailing edge), and periodic condition.

On the nacelle surface and on the blade surfaces, tangency should be satisfied. This is accomplished by specifying the appropriate contravariant velocities, V and W equal to zero, in the case of the nacelle surface and the blade surfaces, respectively.

For an outflow condition, the generalized Riemann invariants are used to determine the variables. The generalized Riemann invariants are given by

$$R_1 = U - [2c/(\gamma - 1)] \quad \text{and} \quad R_2 = U + [2c/(\gamma - 1)] \tag{2}$$

Since R_1 and R_2 are associated with the two characteristic velocities $U + c$, and $U - c$, $U + 2c/(\gamma - 1)$, S, V, and W are determined from the freestream values and $U - 2c/(\gamma - 1)$ are linearly extrapolated from the interior, where $c = \sqrt{\gamma p/\rho}$, $S = \ln(p/\rho^\gamma)$.

The freestream condition is specified before the start of the calculations.

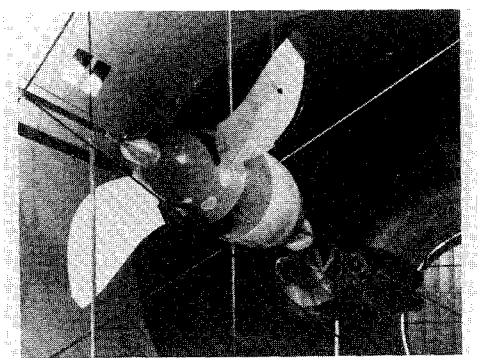

Fig. 4 SR-7L prop-fan model installed in wind tunnel.

Grid System

A computational grid for calculating the flowfield around the prop-fan is generated by using an algebraic method.

The basic blade geometry for the SR-7L prop-fan is shown in Fig. 2. This figure shows the thickness, h/b, blade planform or chord ratio, b/D, sectional design lift coefficient C_{LD}, twist angle $\Delta\theta$ and cone angle ψ as a function of fractional radius, r/R. The airfoils used at each radial location are also indicated in this figure. It can be seen that NACA Series 65 Circular Arc (CA) are used from the root of the blade at $r/R = 0.2$ to the $0.36r/R$ station. At locations between $0.563r/R$ and the tip of the blade, NACA Series 16 airfoils are used. In the region between $0.36r/R$ and $0.563r/R$, transition airfoils are used to blend the characteristics of the Circular Arc and Series 16 airfoils.

In order to generate a grid system around such a complicated configuration, the procedure consists of three steps. Step one is composed of dividing the domain into many axisymmetric parts. Step two consists of generating a two-dimensional H-type grid around the airfoil which is the cross-sectional form of the blade. The final step consists of optimizing the above grid system by utilizing the Poisson equations, and connecting the two-dimensional grids radially. Then, the

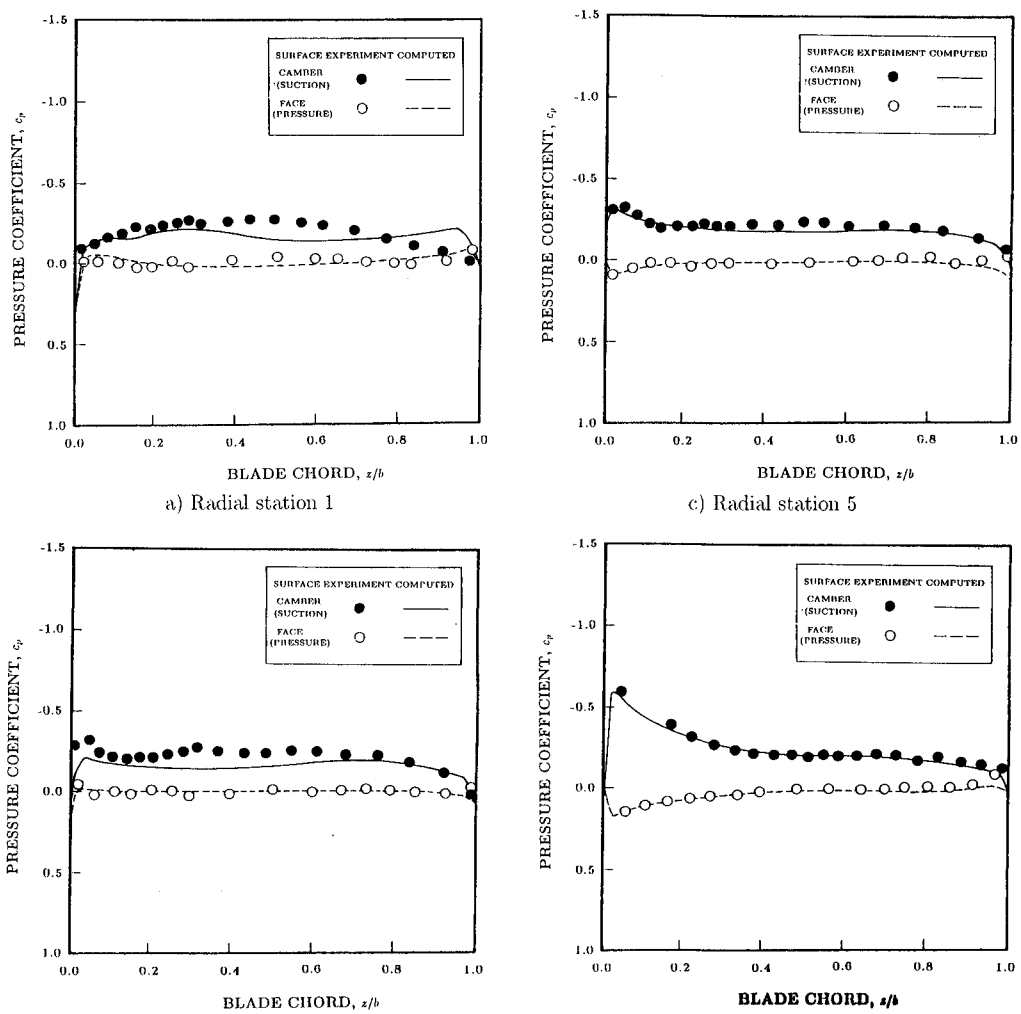

Fig. 5 Comparison of pressure distributions of condition 8.

generation of the three-dimensional grid system is complete. Figure 3 shows the grids generated around the SR-7L.

Wind-Tunnel Test Results

The data used for comparison with the Euler Code calculations was obtained on a specially instrumented blade of the SR-7 prop-fan which was designed for flight test on a modified Lockheed Jetstar in the NASA funded Large Scale Advanced prop-fan (LAP) test program.

Tests were conducted in the S1-MA Large Wind Tunnel at the Modane-Avrieux Aerothermodynamic Test Center operated by the Office National D'Etudes et des Recherches Aerospatiales (ONERA) in France. The prop-fan was driven by Twin Turbomeca gas turbine engines driving a common gearbox. Due to power limitations of the drive engines, the SR-7L could be tested with only two of the eight blades normally installed (Fig. 4). This allowed operation at power loadings per blade similar to those that would occur at takeoff and cruise conditions in an eight-blade configuration. Tests were conducted at the 13 operating conditions.

For this paper the data obtained at test conditions 8 and 12 are used. The former is the condition which most closely approximates the design cruise condition of the SR-7L. At this design condition viscous effects should be a minimum, so Euler Code results have the potential for good agreement.

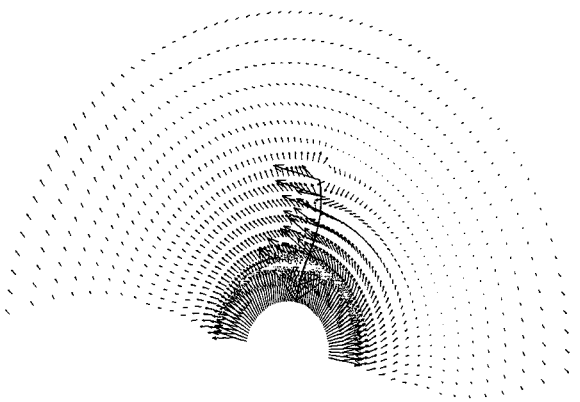

Fig. 6 Vector plots of flow velocities of condition 8.

Results and Discussions

For the numerical simulation the flowfield around the SR-7L prop-fan is calculated through the analysis described in the previous sections. In this calculation the numerical results and the experimental data are compared at conditions 8 (blade angle $\beta = 54.95 \pm 1.00$ deg) and 12 ($\beta = 54.97 \pm 1.00$ deg). Freestream Mach number is 0.5 and 0.78 and advance ratio is 3.055 and 3.07, respectively. The experiment was conducted by using two-bladed prop-fan model. Therefore, calculation is performed for two blades.

The computational space is assumed as follows: the inflow and outflow boundaries are located at 5 tip radii upstream and downstream of the blades, and the outer boundary is two radii from the axis of prop-fan rotation. A total of 101 points in the axial direction, 30 points in the radial direction, and 31 points between adjacent blades in the circumferential di-

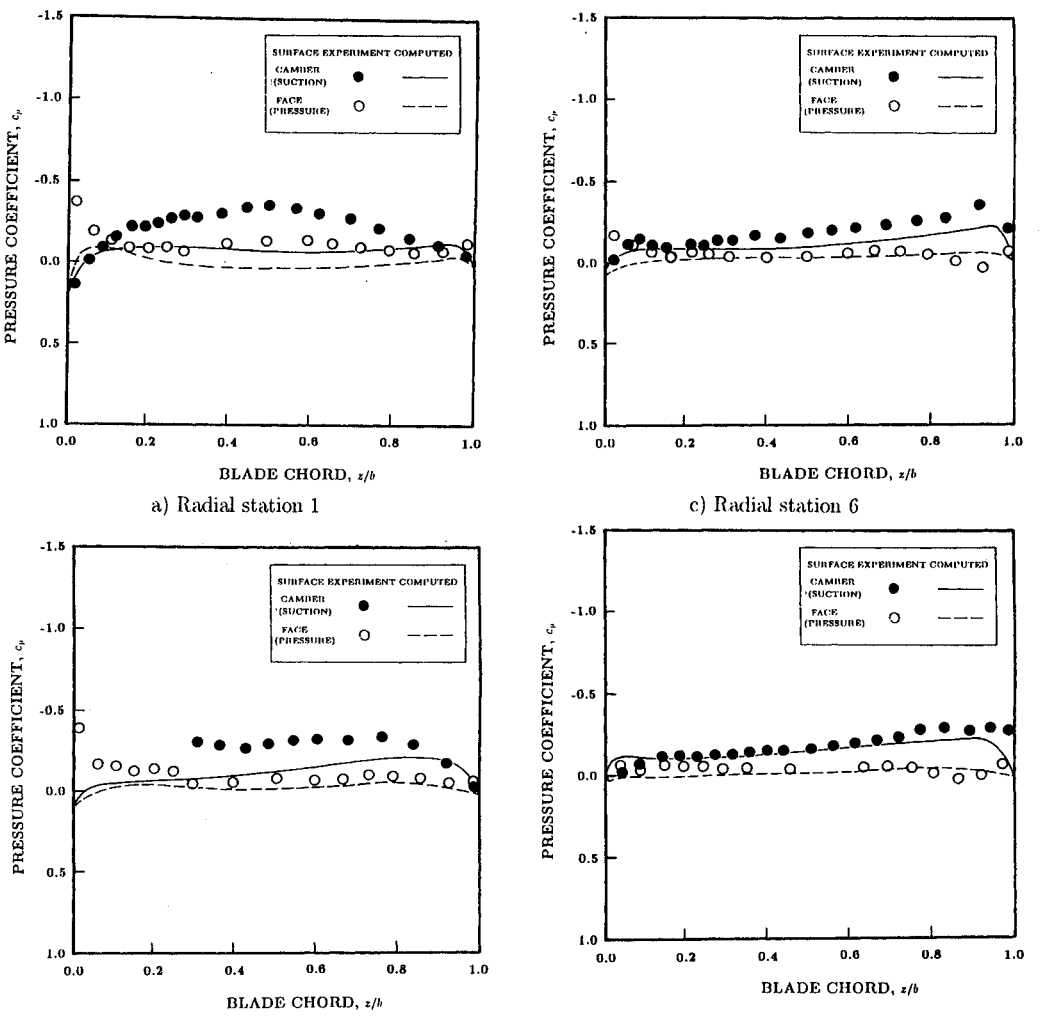

a) Radial station 1

c) Radial station 6

b) Radial station 3

d) Radial station 9

Fig. 7 Comparison of pressure distributions of condition 12.

rection were used for the calculations. On the blade 61 points in the chordwise direction and 16 points in the spanwise direction were used. The blade should be deformed due to centrifugal and aerodynamic loads during operation in the experiment. In the calculation it was assumed that the geometry shown in Fig. 2 accounted for this deformation.

In Fig. 5 the calculated and measured pressure distributions on the blade are compared at 4 stations (radial stations 1, 3, 5, and 10) for the $0.5M_\infty$ case. The lines of the calculated distribution are coincident with the pressure tap lines in the experiment. The computed power coefficient $C_P = 0.34$ at the blade angle $\beta = 54.95$ deg is in good agreement with the experimental result, $C_P = 0.36 \pm 0.020$.

At the radial station 1 the computed pressure distribution differs from the experimental values. This is due to the difference between computed and real prop-fan blade-spinner junction. At the radial stations 3, 5, and 10 the computed pressure distributions show good agreement with the experimental values. Vector plots of the flow velocities just after the trailing edge are depicted in Fig. 6. Tip vortex from the blade is clearly seen in this figure.

For the higher Mach number condition 12 the calculation was also performed. This was the highest power that could be run at the 0.78 Mach number condition. The computed power coefficient, $C_P = 0.23$ at $\beta = 52.95$ deg shows good agreement with the experimental value. At this C_P the calculated pressure distributions on the blade surfaces are shown in Fig. 7. At this condition the blade is slight negative. The pressure distributions of Fig. 7 are seen to be in general agreement with the experimental results. It can be seen in the data that there is a pressure discontinuity at the trailing edge of the blade where a shock is expected due to the supersonic condition caused by the combination of flight and rotation Mach number. This shock was calculated quite well as shown in Fig. 7, at radial station 9.

Concluding Remarks

In order to verify the applicability of the Euler Code to prop-fan aerodynamic design, the flowfield around the two-bladed SR-7L prop-fan at freestream Mach number 0.5 and 0.78 was calculated. The algorithm used in the present analysis was the TVD scheme, which is excellent in shock capturing. Furthermore, an ADI algorithm was adopted together with the TVD scheme.

For condition 8 (freestream Mach number is 0.5) the power coefficient computed by use of the present analysis shows good agreement with that obtained in the experiment. The computed pressure distributions on the blade surfaces agree fairly well with the experimental data. For condition 12 (Mach number is 0.78) the power coefficient computed also shows good agreement with the experimental value. The computed pressure distribution on the blade surfaces in this case shows general agreement with the experimental data.

Therefore, the validity of the present Euler Code for use in aerodynamic design of the prop-fan is verified for the design condition and other high speed conditions. However, at the takeoff condition it is expected that a Navier-Stokes analysis will be required to model the complex flow around a prop-fan blade.[8]

Acknowledgments

The authors wish to acknowledge the many contributions made to the work reported in this paper. NASA Lewis is acknowledged for supporting the acquisition of the test data on the SR-7 and the reduction of the test data. The Hamilton Standard team, who built the special instrumented blade and acquired and processed the data, are also acknowledged. Without dedicated effort from all who were involved, there would be no data available for comparison with calculations.

References

[1]Kobayakawa, M., and Onuma, H., "Propeller Aerodynamic Performance by Vortex Lattice Method," *Journal of Aircraft*, Vol. 22, No. 8, 1985, pp. 649–654.

[2]Kobayakawa, M., et al., "Calculations of High Speed Propeller Performance Using Finite Difference Methods," *Proceedings of 15th Congress of the International Council of the Aeronautical Sciences*, 1986, pp. 1451–1460, 1986.

[3]Kobayakawa, M., and Hatano, I., "Flow Field Around a Propeller by Navier-Stokes Equation Analysis," AIAA Paper 88-3150, 1988.

[4]Campbell, W. A., et al., "A Report on High Speed Wind Tunnel Testing of the Large Scale Advanced Prop-Fan," AIAA Paper 88-2802, 1988.

[5]Chaussee, D. S., and Kutler, P., "User's Manual for Three-Dimensional Analysis of Propeller Flow Fields," NASA Contractor Rept. 167959, 1983.

[6]Bober, L. J., et al., "Prediction of High Speed Propeller Flow Fields Using a Three-Dimensional Euler Analysis," AIAA Paper 83-0188, 1983.

[7]Yee, H. C., et al., "Implicit Total Variation Diminishing (TVD) Schemes for Steady-State Calculations," *Journal of Computational Physics*, Vol. 57, 1985, pp. 327–360.

[8]Wake, B. E., and Egolf, T. A., "Application of a Rotary-Wing Viscous Flow Solver on a Massively Parallel Computer," AIAA Paper 89-0334, 1989.